運輸省港湾技術研究所

港湾技術研究所報告

REPORT OF THE PORT AND HARBOUR RESEARCH INSTITUTE

MINISTRY OF TRANSPORT

VOL. 29 NO. 4 DEC. 1990

NAGASE, YOKOSUKA, JAPAN

港湾技術研究所報告 (REPORT OF P.H.R.I.)

第29巻　第4号 (Vol. 29, No. 4) 1990年12月 (Dec. 1990)

目　　次 (CONTENTS)

REPORT OF THE PORT AND
HARBOUR RESEARCH INSTITUTE
Vol. 29, No. 4 (Dec. 1990)

1. Field and Laboratory Measurements of Shear Modulus Profile in Seabed

Mohsen BADIEY*
Kouki ZEN**
Hiroyuki YAMAZAKI***
and Hideo SUZUKI****

Synopsis

Field and laboratory experiments were conducted to measure the shear modulus profile in the seabed at the port of Kawasaki located at Kanagawa prefecture, Japan. In the field exploration, the recently developed Bottom Shear Modulus Profiler (BSMP) was applied to very soft alluvial clay and loose sand layers. The Downhole Method (DM) and the Standard Penetration Test (SPT) were also used to crosscheck the results of the BSMP measurement. In addition, undisturbed clay samples were taken from the investigation site and the shear modulus was evaluated in the laboratory using the Cyclic Triaxial Test (CTT) and the Unconfined Compression Test (UCT). The shear modulus profiles obtained from five different measurements are compared with each other and the applicability of the BSMP is discussed. The BSMP results for a soft alluvial clay and a sand deposit show good agreement with those from the DM and SPT, especially at shallow depths in the seabed.

Key words: Geophysical Exploration, Laboratory Test, Ocean Soil, Shear Modulus, Site Investigation, Wave Propagation

* Assistant Professor, College of Marine Studies, University of Delaware: Formerly Post Doctoral Fellow, Soil Dynamics Laboratory, Geotechnical Engineering Division.
** Chief, Soil Dynamics Laboratory, Geotechnical Engineering Division.
*** Member, ditto.
**** General Manager, Acoustics Laboratory, Ono Sokki Co. Ltd..

港湾技術研究所報告
第29巻 第4号 (1990.12)

1. 海底地盤の剛性率に関する現地および室内実験

モーセン・バディ*，善 功企**，山崎浩之***，鈴木英男****

要 旨

海底地盤の剛性率を測定するための現地試験および室内試験を川崎港において実施した。現地試験では，最近開発されたボトム・シェアモジュラス・プロファイラー（BSMP）を用いて沖積粘土および緩い砂層の剛性率を調べた。また，BSMP の結果と比較する目的で，ダウンホール法 および 標準貫入試験から剛性率を求めた。さらに，乱さない試料について，一軸圧縮試験，繰り返し三軸試験を行い，原地盤の剛性率を推定した。本文では，上記の5種類の方法から得られる剛性率を比較することにより，BSMP の適用性について検討している。軟弱な沖積粘土および緩い砂層に BSMP を適用して求められた剛性率は，特に，地盤の浅い部分において，ダウンホール法および標準貫入試験により求まる剛性率とよく一致した。

キーワード：物理地下探査，室内実験，海底土，剛性率，現地調査，波動

* 助教授 現デラウエア大学（前 STA フェロー，土質部動土質研究室）
** 室 長 土質部動土質研究室
*** 研究官 土質部動土質研究室
**** 部 長 ㈱小野測器音響技術研究所

Contents

1. Introduction

The shear modulus at low amplitude shear strain is one of the essential parameters in evaluating the dynamic responses of seabed and offshore structures to earthquakes, ocean waves and other types of dynamic loading. In the analysis, the shear modulus evaluated from the shear wave velocity which is measured by the geophysical seismic method is commonly used. The crosshole, downhole, uphole, inhole and surface refraction are the typical methods presently used in the field.

In these methods, a variety of different techniques to generate the seismic waves are used. They are grouped into two categories (MacLamore et al., 1978) : (1) explosive sources, which include blasting agents, air guns, gas guns, sparkers and similar devices; and (2) mechanical sources, such as hammers, vibrators and falling weights. In offshore exploration, most techniques to generate appropriate seismic waves are considerably difficult to apply because of the water depth. Furthermore, for the proper installation of equipmnt and holding the borehole verticality in drilling procedure, platforms are used in general for most investigation sites. This yields inevitable cost and time.

Recently, Yamamoto et al. (1986; 1989) have developed a new method to measure the shear modulus profile of the seabed by using the surface (gravity) water waves existing in natural ocean environment. The equipment called the Bottom Shear Modulus Profiler (BSMP) is attractive in the practical use in a sense that it does not need any borehole and artificial seismic wave sources.

The BSMP was used at several sites where the seabeds were composed of sandy deposits and carbonate sediments and its applicability has been confirmed (Badiey et al., 1987; 1988). The applicability of the BSMP to soft clay and loose sand layers, however, has not been examined in detail so far, especially to the seabed near the surface of which was made up of a very soft alluvial clay usually met at the port and harbour areas in Japan.

The purpose of this paper is to investigate the applicability of the BSMP to soft clay and loose sand layers in shallow water depth. Different types of field measurements and laboratory tests are employed to evaluate the in-situ shear modulus : They are (1) the BSMP, (2) the Downhole Method (DM), (3) the Standard Penetration Test (SPT), (4) the Cyclic Triaxial Test (CTT) and (5) the Unconfined Compression Test (UCT).

The in-situ measurements are performed at the port of Kawasaki in Tokyo Bay. The undisturbed samples are also taken from the site for the CTT and the UCT in the laboratory. The evaluated in-situ shear modulus profiles from the different measurements are presented for the comparisons and the applicability of the BSMP is discussed in this paper.

2. Field Experiments

2. 1 Bottom Shear Modulus Profiler

The remote sensing methcd of the BSMP was developed by Yamamoto et al. (1986; 1989). It has been demonstrated that measurements of the seafloor displacement generated by surface waves can be used to determine the shear modulus of the seafloor on the continental shelf (Yamamoto and Torii, 1986, Trevorrow et al., 1987; 1988). This method uses the seabed admittance, which is defined as the ratio of the wave-induced displace-

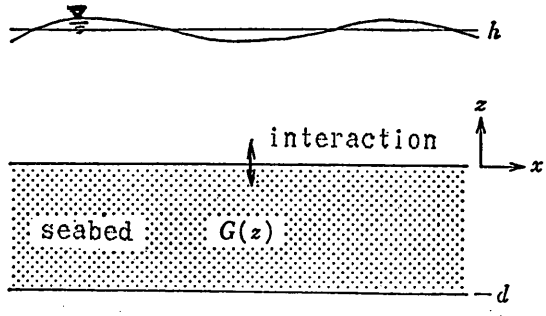

Fig. 1 Gravity water wave and bottom layer interaction model

ment to the wave-induced pressure on the surface of seafloor as input to a linearized inversion scheme for calculation of the shear modulus profile.

The basic theory of the wave-seabed interaction and the theoretical aspects of the BSMP has been published in several papers (Yamamoto, 1983a ; 1983b). Here, we briefly explain the theoretical concept of this method and mainly concentrate on the interpretation of the measured BSMP data in order to examine the practical applicability of the BSMP in comparison with other methods which are presently available in this field.

(1) Theoretical Background

A gravity water wave propagation model used in the BSMP is shown in **Fig. 1.** The direction of the propagation is onto the x axis and the vertical direction is represented by the z axis with $z=0$ at the sea bottom. It is assumed that the water depth h and the shear modulus G (z) do not change in the x direction. At $z=-d$, the bottom layer is connected either to 1) an elastic half space with constant shear modulus, or 2) an ideally rigid boundary. Furthermore, it is assumed that :

1) the coupling between the solid frame and the pore water is perfect,
2) shear deformation is dominant,
3) the inertia due to the layer mass is negligible, and
4) the deformation of the layer is considered linear.

A forward theory for the present problem is to determine the amplitude at the sea bottom due to the water wave when 1) the water depth h, 2) the shear modulus G (z), 3) the gravity water wave pressure $P(0)$ at the sea bottom, and 4) its frequency (or period) are given. A simplified (and mostly accurate) relation between the wave number λ and the frequency f is giveny by

$$gh \tan(\lambda h) = \omega^2 = (2\pi f)^2 \tag{1}$$

where g is the gravitational acceleration. This relatioin determines the wave number λ for a given water depth and frequency of a water wave.

The relation among the horizontal displacement u, vertical displacement v, compressional stress τ_{zz}, and shear τ_{xz} of the bottom layer due to the water wave is described by the coupling matrix (Yamamoto et al., 1986, 1989).

$$\frac{d}{dz}\begin{pmatrix} r_1 \\ r_2 \\ r_3 \\ r_4 \end{pmatrix} = \begin{pmatrix} 0 & \lambda & 1/G & 0 \\ -\lambda & 0 & 0 & 0 \\ 4G\lambda^2 & 0 & 0 & \lambda \\ 0 & 0 & -\lambda & 0 \end{pmatrix}\begin{pmatrix} r_1 \\ r_2 \\ r_3 \\ r_4 \end{pmatrix} \tag{2}$$

where a stress-displacement vector $r\ (z)=[r_1,\ r_2,\ r_3,\ r_4]$ is used and

$$\left.\begin{aligned} &u=ir_1\theta, \qquad v=r_2\theta \\ &\tau_{xz}=ir_3\theta, \qquad \tau_{zz}=r_4\theta \\ &\theta=\exp\ [i(\omega t-\lambda x)] \end{aligned}\right\} \tag{3}$$

The coupling matrix is composed only of $G\ (z)$ and λ. Eq. (2) is a boundary value problem with two conditions at $z=-d$ and another two at $z=0$. For example, at $z=0$, the shear stress is zero and the compressional stress is equal to the gravity water wave pressure at the sea bottom. By solving Eq. (2) with these conditions, the amplitude of the horizontal and the displacements due to the unit water wave amplitude at $z=h$ (sea level) for different wave period (refered to as admittance $\xi\ (f)$, hereafter) is obtained if the shear modulus profile of the bottom layer is known. The admittance of a sea bottom is measured by use of a seismometer and a pressure sensor.

An inversion problem is a process to determine the unknown shear modulus profile $G\ (z)$ from a measured admittance characteristic $\xi_a\ (f)$. In order to determine the shear modulus $G\ (z)$ from the measured admittance the bottom layer must be divided into M sublayers with unknown shear moduli G_m, $m=1,\ 2,\cdots\cdots M$. An equal or larger number of admittance values ξ_{an}, $n=1,\ 2,\cdots\cdots,N$ $(N\geqq M)$ at different frequencies must be used to uniquely determine G_m. A relation between the admittance ξ and the shear modulus vector G is expressed in a general form:

$$\xi=f(G) \tag{4}$$

This can be linearlized by the Taylor expansion,

$$\begin{aligned} \xi-f(G_{init}) &\approx\left(\frac{\partial f(G)}{\partial G}\right)_{G=G_{init}}(G-G_{init}) \\ &\approx\left(\frac{f(G+\Delta G)-f(G)}{\Delta G}\right)_{G=G_{init}}(G-G_{init}) \end{aligned} \tag{5}$$

where G_{init} is an initially assumed shear modulus profile. The left hand side of Eq. (5) is interpreted as the difference between the measured admittance values and the calcualted admittance values from initial shear modulus values at different wave periods $(\xi_{an}-\xi_{cn})$. The first parenthesis of the right hand side is a rate of increase of the nth admittance $(n=1,\ 2,\cdots\cdots,\ N)$ when the shear modulus of the mth sublayer is increased by ΔG_m $(m=1,\ 2,\cdots\cdots,\ M)$ $((\xi_{cnm}-\xi_{cn})/\Delta G_m)$. These rates $(N\times M)$ are all calculated from the forward theory. The second parenthesis is the difference between the new and initial shear modulus values. By solving Eq. (2) $(N\times M$ overdetermined simultaneous eqution$s)$, values of new shear modulus are obtained for each sublayers. These will be used for the next trial.

A flow chart of determining the shear modulus from the measured admittance is shown in **Fig. 2.** Steps are as follows:

1) reliable number of measured admittance data (N) are read from the date file.
2) the bottom layer is divided into M $(M\leqq N)$ sublayers and the boundary at $z=-d$ is specified.
3) initial shear moduli for each sublayers are given.
4) using the forward theory, the calculated admittance is compared with the measured admittance.
5) if the error is large, the initial shear moduli are modified using the inverse theory, and goes back to step (4).
6) steps (4) and (5) are repeated until the error is small enough or until no further improvement is achieved.

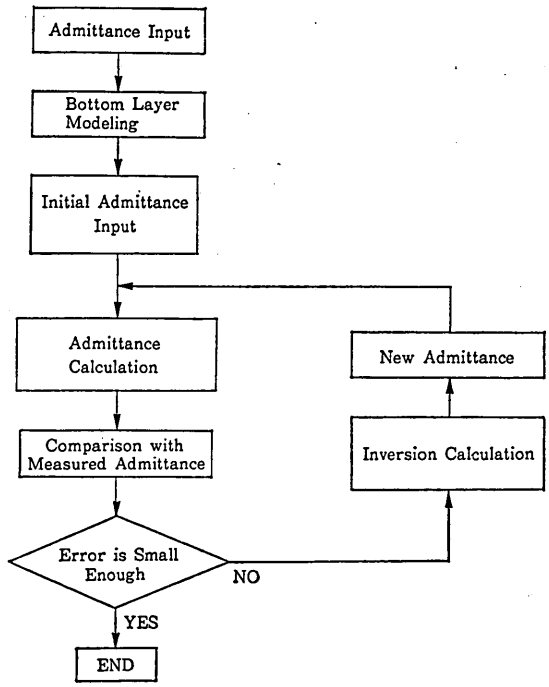

Fig. 2 Flow chart of the shear modulus analysis from measured admittance data

The shear modulus of soils is known to be strongly dependent of the applied shear strain amplitude (Seed and Idriss, 1970). Namely, it decreases drastically in accordance with the increase of the shear strain amplitude because of the non-linearity of stress-strain hysteresis of soils. It is, therefore, important to define the shear strain amplitude where the shear modulus is measured. The generated shear strain amplitude in the conventioal geophysical seismic methods such as the Downhole and Crosshole Method, is not directly measured but it is empirically considered to be less than 10^{-6}. Below this strain, the soil element in the seabed behaves like an elastic material, indicating a constant shear modulus irrespective of the shear strain. In the BSMP measurement, the shear strain amplitude is also very small, because the motion or displacement of the seabed induced by ocean waves is infinitesimal. Then, the shear modulus, G, treated in this study corresponds to one at low amplitude of shear strain less than 10^{-6}. The G will be denoted by the G_o, hereafter.

(2) Instrumentation and Data Collection

The existing Bottom Shear Modulus Profiler (BSMP) consists of three orthogonally mounted seismometers in a water proof housing and a pressure transducer. The function of the seismometers is measuring seafloor motion induced by the propagating surface (gravity) waves. The pressure transducer measures the weve-associated oscillatory pressures at the surface of the seabed. The block diagram of this system is shown in **Fig. 3.**

The housing of the BSMP is a hollow stainless steel cylinder with dimensions given in **Fig. 4.** The seismometers, the data logger and recording unit are mounted in this housing. The pressure transducer is mounted vertically on the base and the sensing element of this unit is exposed to the outside via a mesh plate which protects the surface against any external damages. Inside the housing, there are two pendulum inclinometer to measure

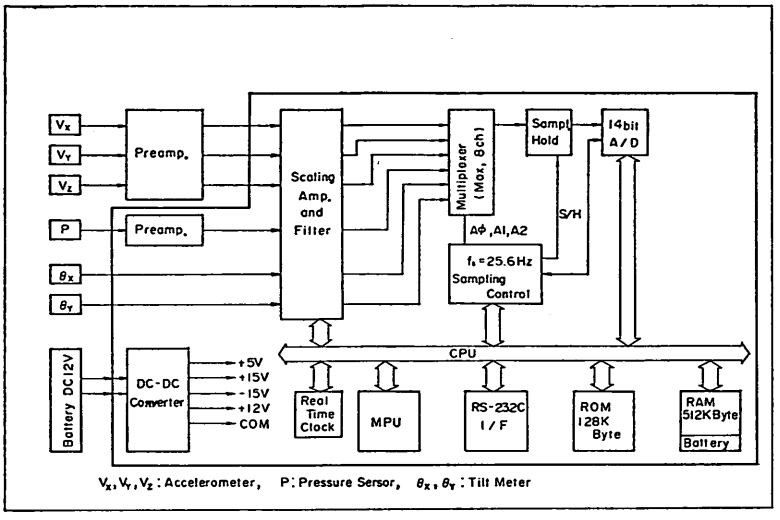

Fig. 3 Block diagram of the BSMP

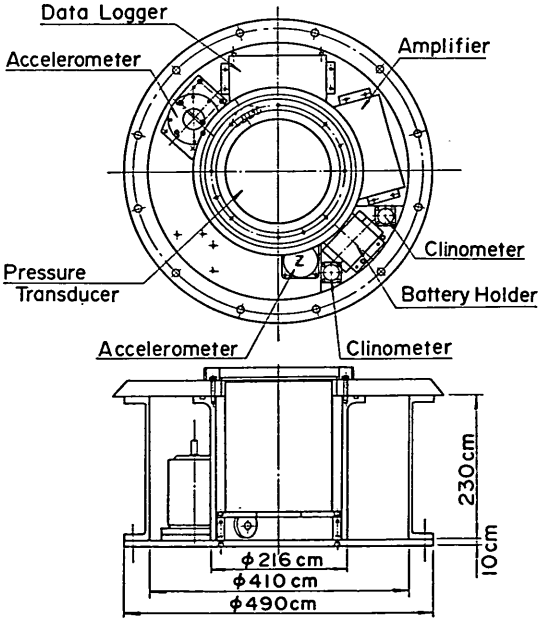

Fig. 4 Housing configuration of the BSMP

the inclination of this housing when placed on the seafloor. The total weight of the BSMP is about 100kgf.

Using a piezoelectric sensor, the seismometers measure the acceleration of the seafloor motion under the gravity water waves. The piezoelectric snesor is attached to the frame of the seismometer housing and to a suspended mass. Seafloor motion causes a relative movement between the frame and the suspended mass. This movement induces a strain

in the piezoelectric sensor and produces a charge which is converted into a voltage signal. The signal which is the seafloor acceleration is then amplified and filtered by a board inside the seismometer. Since a flexible retaining disc is attached to the bottom of the suspended mass and the seismometer sensor, this particular sensor can be used at any inclination and is insensitive to the off-axis ground motion. In addition, this sensor is filled with a viscous oil to increase damping of the system. The seismometers used in this experiment were Teledyne-Geotech Model S-510. It has a low cut-off frequency (−3dB) of around 0.05Hz (20s) and approximately −1dB decrease in response at 0.1Hz. This response at the low frequency end must be compensated in the analysis. The high cut-off frequency is much higher than 10Hz.

The differential pressure transducer used for the BSMP system is designed to detect pressure oscillations of the water gravity waves in the ocean environment for a low frequency range of 0.01Hz to 1Hz (Cox et al. 1984). This range encompasses the pressures generated by the surface (gravity) waves, the seismic disturbances of the seabed, the microseisms and the low frequency end of the acoustic spectrum. A calibration of the pressure sensor was made by lifting or lowering it by a fixed height in a short period of time in a water tank. The measurement showed that the low cut-off frequency (−3dB) of this sensor was approximately 0.005Hz.

The system used here has a self contained memory package which enables the users to record approximately four hours of uninterrupted data. The data is sampled at 25.6Hz through a self-contained memory unit which was designed to record the data inside the housing independent of the attending ship. The specifications of this storage unit are given in **Table 1**.

The date is collected in several blocks. Each block contains 1024 points or about 400 seconds at the provided sampling rate. An automatic range gain is installed into the data logger which will be set once the system is in the water and settled on the seafloor. If the conditions of waves change during the course of a measurement, this device can adjust the new gains and retain the original values for the adjustments. The data logger also contains a multiplexer board, scaling amplifiers and filters (see **Fig. 3**). After the data is recorded, the housing is retrieved and the data is transferred from the memory unit to diskettes via a personal computer.

The three stages of the installation, measurement and recovery are schematically drawn in **Fig. 5**. In stage (a), the self-contained BSMP system is lowered from the ship along with the anchor which is hooked to a buoy via a steel cable. This cable is used later in order to recover the system after measurements. In stage (b), the system is left on the ocean floor for the period of up to four hours for recording the data. Finally, in stage

Table 1 Specifications of the self-contained memory unit

Component	Specification
A/D board	14 bit
MPU	Motorola 6800
ROM	128 kbyte
RAM card	512 kbyte
Spectrum line	400
Frequency resolution	0.0025 Hz.
Maximum block number	32
1 block length	400 seconds
1 block sample number	1024

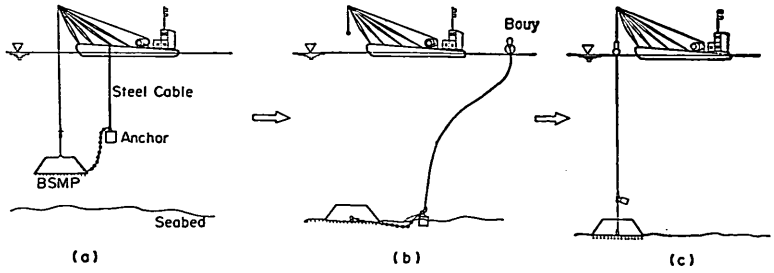

Fig. 5 Installation of the BSMP; (a) deployment, (b) data collection, (c) equipment recovery

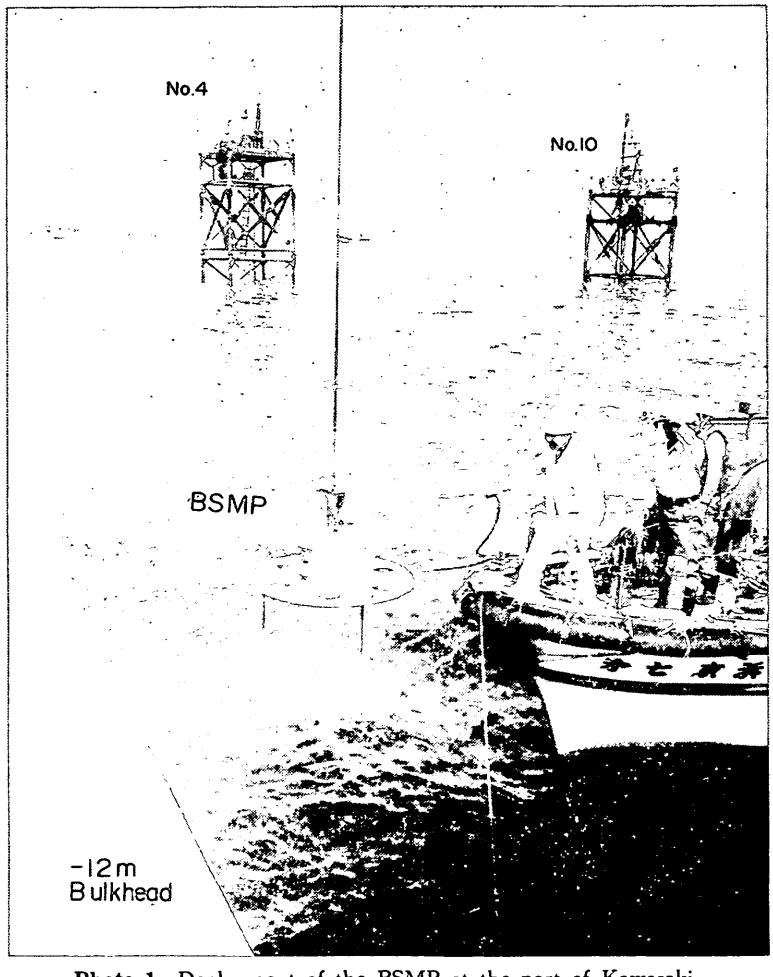

Photo 1 Deployment of the BSMP at the port of Kawasaki

(c), the system is removed from the ocean floor by a steel cable. **Photo 1** shows the BSMP deployment during the installation.

(3) Data Analysis

As an examples of the raw data stored in the memory, one block of the pressure and

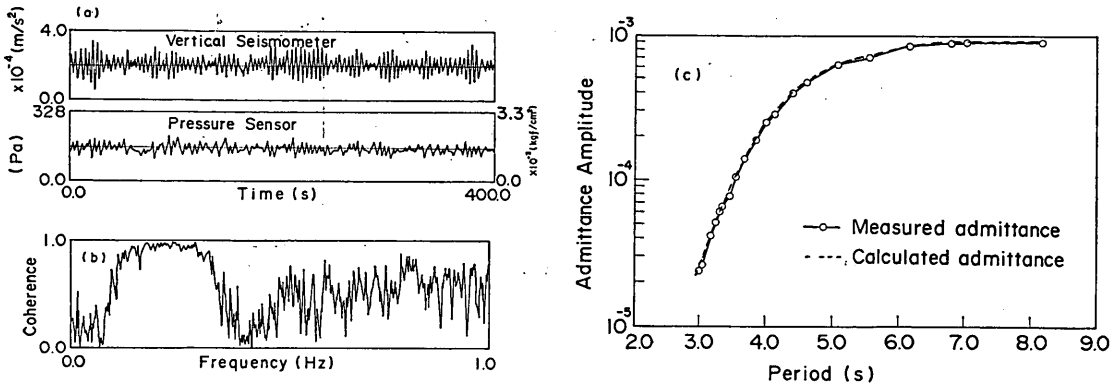

Fig. 6 Data processing; (a) raw seismic and pressure data, (b) coherence between vertical seismometer and pressure signal, (c) calculated and measured admittance

the acceleration signals are shown in **Fig. 6(a)**. **Fig. 6(a)** shows the vertical seismometer and the pressure sensor signals versus time for 1024 data points. From the similarity between the two signals it is seen that they are correlated. This is confirmed by use of the FFT (Fast Fourie Transform) technique. Both the pressure and the accelaration signals are discrete Fourier transformed, and the autopower spectra (S_{pp}, S_{aa}) of individual signals and the cross-power spectra (S_{pa}) of the two signals are obtained. A coherence function ($\gamma^2 = |S_{pa}|^2 / S_{pp}\, S_{aa}$) is calcualted at the same time to check whether there is a correlation between the pressure and the acceleration signals. **Fig. 6(b)** shows one example of coherence as a function of frequency. A large coherence (usually larger than 0.95) indicates that the signals are higher than the noise level and that the acceleration is caused by the water pressure and that the relation between the pressure and the accelaration is linear. The autopower spectrum of the pressure signal S_{pp} also indicates the frequency band where there is a significantly large gravity water waves. Normaly, the frequency band ranges from 0.05Hz to 0.25Hz (from 20s to 4s in period) in the water of depth within 100m. The transfer function between the pressure and the acceleration signals (S_{pa}/S_{pp}) gives the admittance characteristic when multiplied by a frequency dependent coefficient. Only the admittance data in the frequency band with high coherence is used as the input data for the inversion analysis (see **Fig. 2**). **Fig. 6(c)** shows an example of measured admittance data as a function of period by circles. A curve shown by the dotted line in **Fig. 6(c)** is a calculated admittance by inversion. The measured and calculated admittances show a good agreement indicating that the inversion scheme worked well in this case. The number of blocks and wave data used for the analysis are tabulated in **Table 2**.

Table 2 Number of blocks and wave data used for the analysis

No.	Point	Date	Water depth(m)	No. of blocks	No. of waves	Other measurements
1.	KW1	29 June, '89	10.5	12	20	UCT, CTT, DM, SPT
2.	KW2	29 June, '89	14.0	7	20	none
3.	KW3	30 June, '89	13.0	18	20	none
4.	KW4	30 June, '89	14.8	11	20	none
5.	KW5	01 Jnly, '89	10.4	11	20	SPT, DM, UCT, CTT
6.	KW6	03 July, '89	13.2	14	20	none

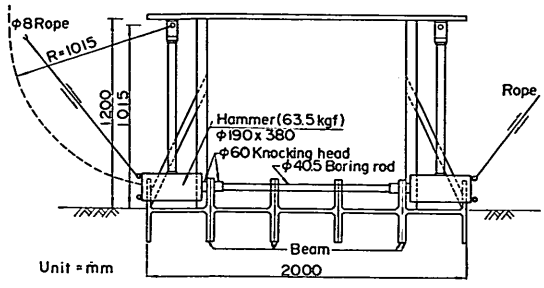

Fig. 7 Shear wave generator for Downhole Method

2. 2 Standard Penetration Test

The shear modulus at the low amplitude of shear strain, G_o, can be estimated from the very common method of the Standard Penetration Test (SPT). The number of blows, N, is empirically related to the shear modulus:

$$G_o = aN^b \quad (\mathrm{kgf/cm^2}) \tag{6}$$

where a and b are the constants. The values of the constants reported so far lie between 100 and 158 for the a and between 0.62 and 0.8 for the b (Ishihara, 1976). In this study, the values of $a=120$ and $b=0.8$ presented by Ohsaki and Iwasaki (1973) are adopted to estimate the shear modulus from the N-value. The shear modulus measured with the BSMP will be compared to discuss with that estimated from the SPT in the later section.

2. 3 Downhole Method

The Downhole Method (DM) was used for the measurement of the in-situ shear modulus of the seabed as a comparative method with the BSMP. The measurements were performed at two boreholes. As the clay at the surface of the seabed was so soft like a slurry that the equipments for the shear wave generation were specially prepared as shown in **Fig. 7** and placed near the boreholes. The reversible mechanical seismic source for the shear wave was attained by installing the drive hammer on both ends of the steel plate and dropping them, alternately. For the compressional wave, it was attained by hitting the boring rod up and down. The receiver (three dimensional velocity transducer) was wedged in the vinyl chloride casing. According to the elastic wave equation, the shear modulus is calculated from the following equation;

$$G_o = \frac{10}{9.8}\gamma_t V_s^2 \quad (\mathrm{kgf/cm^2}) \tag{7}$$

where, γ_t (gf/cm^3) is the unit weight of soil, V_s (m/s) is the shear wave velocity.

2. 4 Experiment Site and Soil Profile

The Bottom Shear Medulus Profiler (BMSP) and the Downhole Method (DM) were used for the in-situ measurements of the shear modulus profile at the port of Kawasaki located at Kanagawa prefecture, Japan (**Fig. 8(a)**). This location was in the area of the expansion project of the berth Nos. 7 and 8 and was currently under the soil investigation for the design of facilities.

The experiment site is bounded by two breakwaters with a 450 meter of the opening as shown in **Fig. 8(b)**. The incident waves enter this bounded area through an oblique angle. Water wave propagation at this location becomes further complicated after the

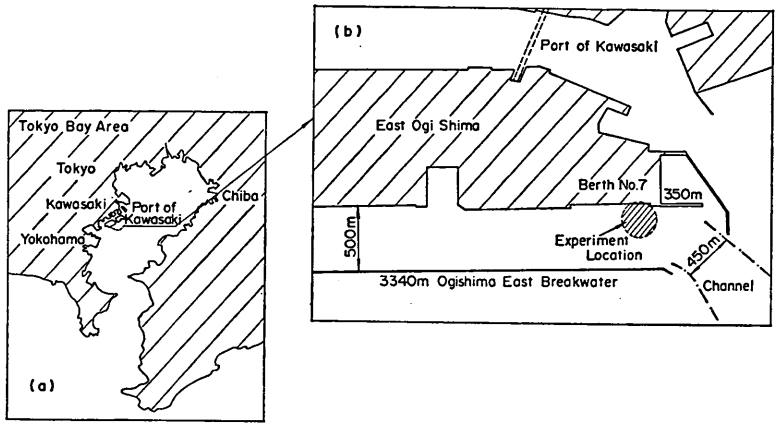

Fig. 8 Location; (a) the port of Kawasaki, (b) experiment site

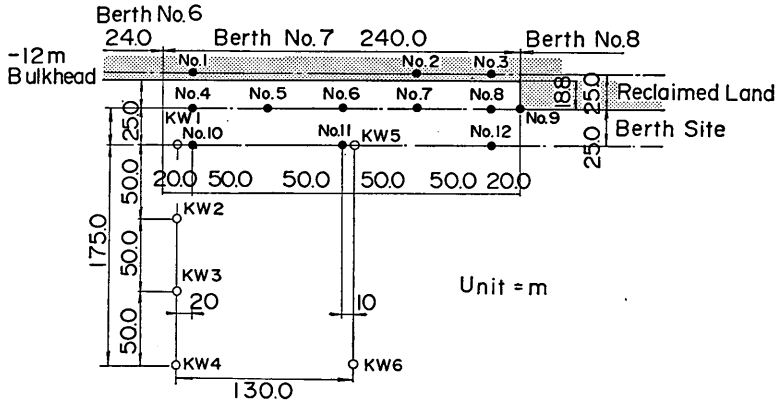

Fig. 9 Points of the BSMP measurement

waves are reflected from the seawall. Therefore, the measured wave-induced sea bottom pressure may be affected by this geometry, since there is a combination of oblique incident waves. The reflected waves from the seawall can change the dispersion relationship of the gravity water waves given by Eq. (1). This, in turn, will exert an effect on the wave-induced seabed motion and cause some difficulties in the interpretation of the results. This will be discussed in more details in later chapter.

Fig. 9 shows the dimensions of the experiment site along with the BSMP experiment points denoted by KW1 to KW6. The solid circles numbered 1 through 12 shown on **Fig. 9** are the locations where the soil investigations were performed separately from the BSMP measurement. For our comparative study, the DM and SPT as well as the sampling of undisturbed clays were conducted at the borehole Nos. 10 and 11 respectively close to KW1 and KW5.

The soil profile of the seabed between borehole Nos. 10 and 11 are presented in **Fig. 10**. As shown in **Fig. 10**, the seabed at borehole No. 10 is an intact layer consisting of several alluvial and diluvial clays. Whereas, at borehole No. 11 there exists sand deposits down to -30m from the mean sea level. According to the construction record, the clay at the borehole No. 11 and its vicinity was replaced with sand several years ago. The N-values of the artificially replaced sand are less than 10 as illustrated in **Fig. 10**, but the hard stratum

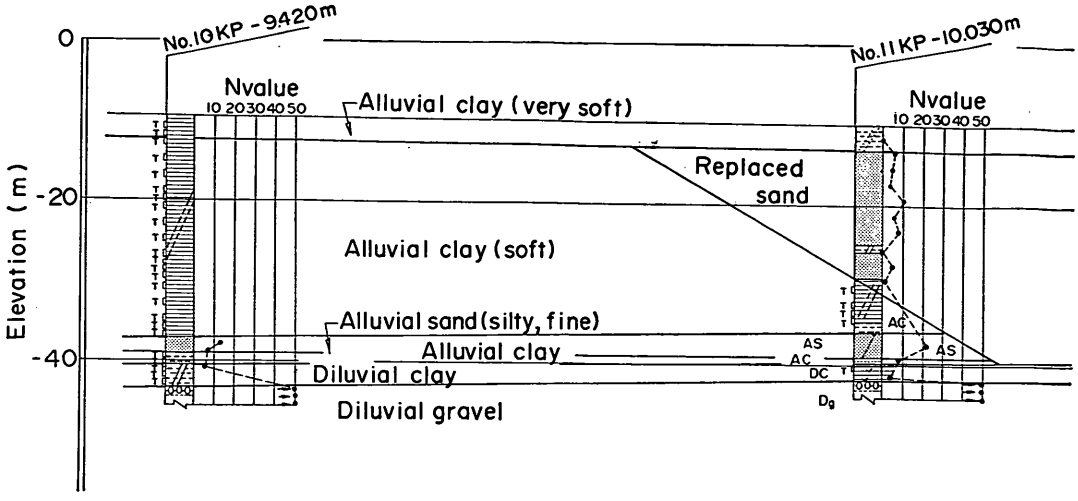

Fig. 10 Soil profile

whose N-value is more than 50 is found below the elevation of -42m. So, the measurements are focussed on the soft layers above that depth.

3. Laboratory Experiments

3. 1 Physical Properties of Samples

The undisturbed samples for the Unconfined Compression Test (UCT) and Cyclic Triaxial Test (CTT) in the laboratory were taken from the borehole Nos. 10 and 11 near the points KW1 and KW5. The sampling was done with the stationary piston sampler in the intervals indicated by the symbol T in the soil profile in **Fig. 10**. Since the alluvial clay around borehole No. 11 has been replaced by sand, the SPT was executed in this sand layer, instead of the undisturbed sampling.

The physical properties of the samples such as the unit weight of soil, γ_t, water content, w, vold ratio, e, plasticity index, I_p, and specific gravity, G_s, are tabulated in **Table 3** together with the unconfined compressive strength, q_u, and axial strain at failure, ε_f. **Fig. 11** shows

Table 3 Physical properties and strength characteristics

No.	Depth (m)	γ_t (gf/cm³)	w (%)	e	S_r (%)	q_u (kgf/cm²)	ε_f (%)	I_p	G_s
10(T 2)	2.4	1.51	77.5	2.21	95.9	0.13	5.1	32.9	2.73
10(T 7)	10.4	1.45	87.5	2.51	94.9	0.29	8.2	56.4	2.71
10(T13)	19.1	1.39	106.7	2.96	96.1	0.57	7.0	57.2	2.66
10(T17)	26.4	1.80	35.9	1.05	92.8	0.68	3.6	—	2.72
10(T23)	33.4	1.89	30.2	0.87	94.4	1.28	4.2	19.6	2.70
11(T 2)	21.4	1.46	89.5	2.44	97.0	1.22	2.5	50.3	2.64
11(T 6)	25.4	1.72	44.6	1.28	94.6	1.38	4.2	16.5	2.70

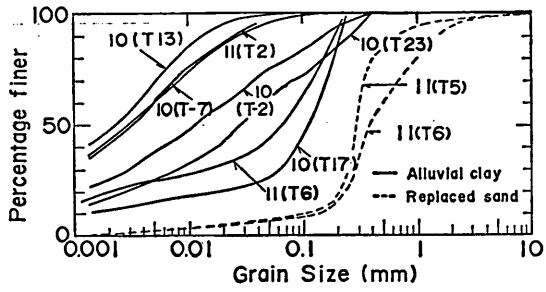

Fig. 11 Grain size distribution curves

the grain size distribution curves in which the numbers correspond to those of boreholes and sampling tubes in **Table 3.** The dotted lines are for the replaced sand at the borehole No. 11. It is found from **Table 3** and **Figs. 10** and **11** that the original seabed in this region mostly consists of clayey soils with the I_p more than 50 but it becomes silty at the deeper depths more than about 25m.

3. 2 Unconfined Compression Test

The Unconfined Compression Test (UCT) was performed according to the Japan Industrial Standard (JIS). The dimension of the specimens was 8cm high and 3.5cm in diameter. The constant axial strain rate of 1.0%/min was applied to the specimens.

The q_u was converted to the shear modulus at the low amplitude of shear strain, G_o, by using the empirical equations proposed by Zen et al. (1987) shown in **Fig. 12**;

$$G_o = 170\ q_u \tag{8}$$

in which the average values of the q_u for the specimens at the same depth are adopted to estimate the shear modulus. The G_o (lab.) and G_o (in-situ) in **Fig. 12** are the shear modulus in the field, respectively evaluated from the CTT and the Downhole Method or the

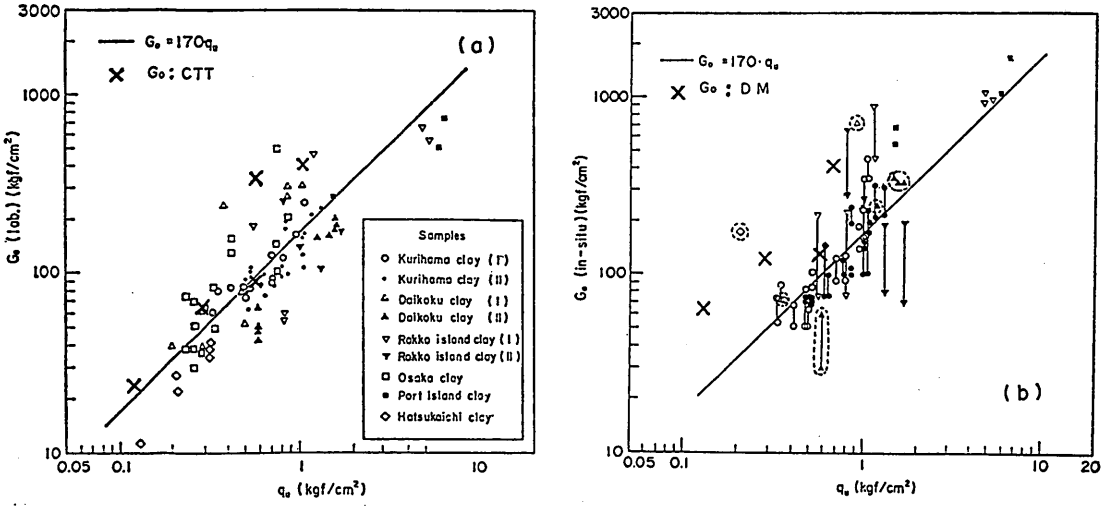

Fig. 12 Unconfined compressive strength and shear modulus; (a) laboratory measurement, (b) in-situ measurement (after Zen et al., 1987)

Crosshole Method. The estimated values from the measurements in this study are plotted in **Fig. 12** together with the data presented by Zen et al. (1987).

3. 3 Cyclic Triaxial Test

The samples for the Cyclic Triaxial Test (CTT) was trimmed to columns of 5cm in diameter and 12cm in height. After the preparation of each specimen, it was set on the pedestal in the triaxial cell and covered with the drain paper and rubber membrane. The back pressure of 1.0kgf/cm^2 was applied to the specimen in order to increase the degree of saturation. Then, specimen was isotropically consolidated under the confining pressure corresponding to the effective overburden pressure in the field. After the completion of the consolidation, the sinusoidal from of the axial load with the period of 10s was repeated and the stress-strain hysteresis curves were recorded. To measure the shear modulus for a wide range of shear strain, the amplitude of the axial load was increased step by step after 10 cycles of the loading at each stage. For the lower range of strains of less than 10^{-3}, a highly sensitive strain gap sensor was used for the precision of the measurement. The data was collected digitally using a personal computer and was analyzed automatically.

The shear modulus obtained from the isotropically consolidated specimens must be corrected, since the in-situ stress conditions are anisotropical. The relationships between the shear modulus at the low amplitude of shear strain (less than 10^{-5}) and the mean principal stress are experimentally found linear as shown in **Fig. 13** (Zen et al., 1987). So, the measured shear modulus, G_o (lab.), under the confining pressure corresponding to the effective overburden pressure in the field is corrected to the in-situ shear modulus, G_o (in-situ), by the following equation;

$$G_o(\text{in-situ}) = G_o(\text{lab.})\frac{(1+2K_o)}{3} \tag{9}$$

where K_o is the coefficient of earth pressure at rest. In this study, the K_o of 0.5 is assumed.

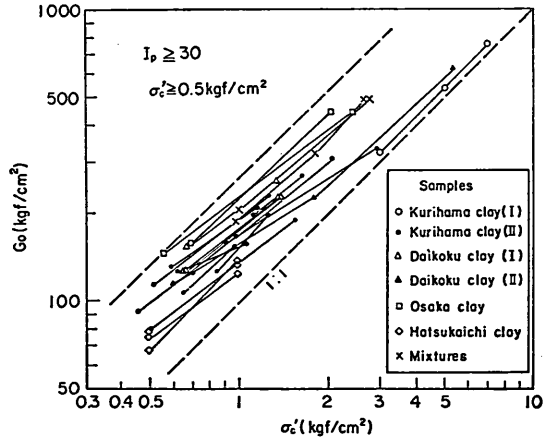

Fig. 13 Effective mean principal stress and shear modulus (after Zen et al., 1987)

4. Results and Discussions

4. 1 Comparisons of Shear Modulus

Fig. 14 is the comparison of the shear modulus profiles at the point KW5 where the seabed is composed of the replaced sand. The solid circles are estimated results from the N-values using Eq. (7) and the solid triangles are those from the DM. The results of the BSMP is denoted by the open circles. As can be seen from **Fig. 14**, the shear modulus profiles of the replaced sand indicate a fairly good agreement each other, irrespective of the different measurements. Experiments in some other areas in Japan have also shown that the BSMP and SPT results agree very well (Suzuki et al., 1990). On the other hand, the comparisons of the shear modulus profiles of the alluvial clay layers below the depths of 18m show a poor agreement. The reason of this poor agreement will be discussed later on.

Fig. 15 shows the comparisons of the shear modulus profiles of the alluvial clay layers measured by the BSMP at the points KW1 and KW4 with those measured by the DM. The results of the UCT and CTT in the laboratory are also presented in **Fig. 15** in which Eq. (8) is adopted to estimate the in-situ shear modulus from the unconfined compressive strength, q_u, and the shear modulus from the CTT is plotted for the shear strain amplitude, $\gamma=10^{-6}$ and 10^{-5}. The profiles obtained from the UCT compare fairly well with those from the CTT. While, both the laboratory test results are a little smaller than the in-situ measurements. The reason for this is that the sample disturbance would bring about the reduction of the shear modulus. The samples taken from the deeper layers had a lower plasticity index and were either expanded or cavitated under no confining pressure conditions during the preparation of specimens. Okumura (1974) presented that the effect of the sample disturbance on the modulus of deformation is one order larger than that on the shear strength.

The comparison between the BSMP and DM results shows that the differences are considerably large, especially at the deeper depths. The values show an increasing deviation trend of the shear modulus with depth. When it is limited to the shallow depths down

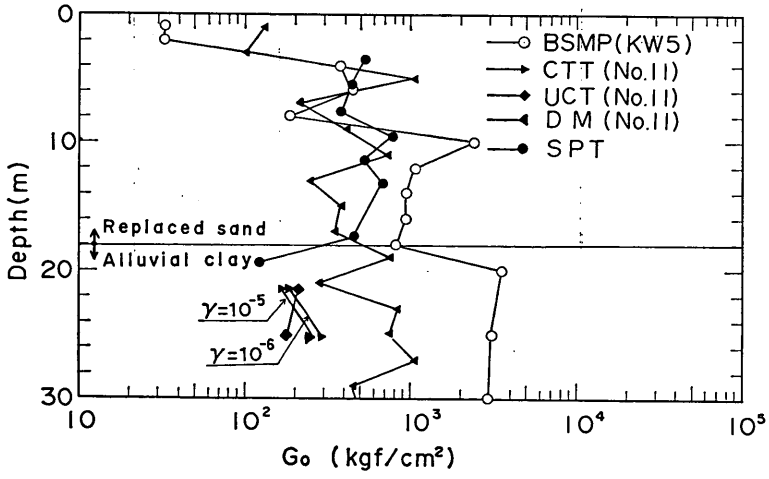

Fig. 14 Comparison of the shear modulus profiles (replaced sand layer)

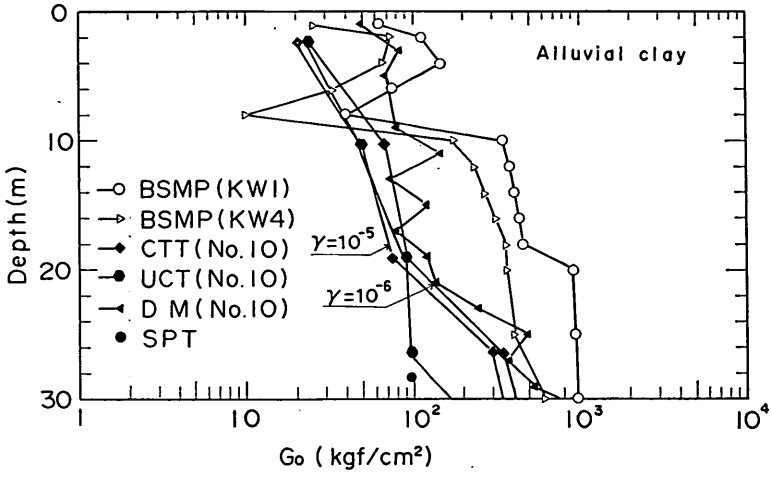

Fig. 15 Comparison of the shear modulus profiles (alluvial clay layer)

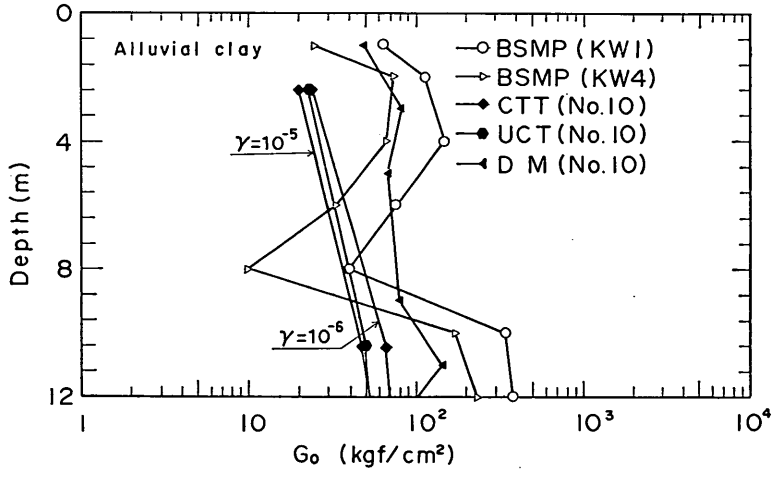

Fig. 16 Shear modulus profiles at the shallow depth (alluvial clay layer)

to 10 meters from the seabed, however, the profiles appear to compare more favourably with the DM results as illustrated in **Fig. 16**. This is the same inclination as observed in **Fig. 14**. The depth resolution of the BSMP data depends on the periods at which the wave spectra of pressures as well as the seismometer signals are coherent. The longer waves penetrate deeper and the shorter waves can give a better resolution for the surface layers. The reason for the deviation trend of the shear modulus profile from the others is considered that the location of the BSMP experiment is bounded by two breakwaters and the land on one side. The geometry does not allow for any high amplitude or long waves to propagate into the experiment site, so that the resolution of the data is limited only to the shallower depths of the seabed (down to about 10m from the seafloor for this site).

Fig. 17 is the comparison of the shear modulus measured with the BSMP and DM. In **Fig. 17**, only the results at the shallow depths are plotted. The open circles are for the replaced sand layer and the solid circles are for the alluvial clay layer. It is recognized

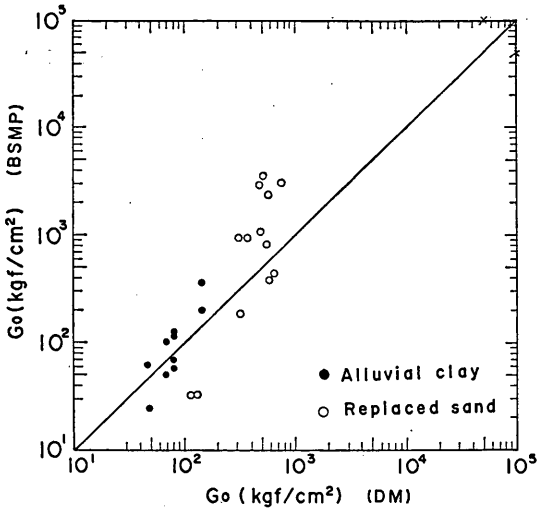

Fig. 17 Comparison between the BSMP and DM measurements

from **Fig. 17** that the shear moduli measured with the BSMP compare well with those evaluated from the DM.

4. 2 Effect of Geometry on BSMP Results

The location of the experiment at the port of Kawasaki is bounded by East Ogi Shima (island) and two breakwaters as shown in **Fig. 8**. Due to the complicated geometry of this location, the waves undergo a refraction upon their entrance to the inlet and reflection from the seawall after they propagate inside. This may lead to some effects on the analytical results. Several points should be noted in order to examine the quality of the collected data set of the BSMP affected by the geometry. The data were therefore collected at total of six points from KW1 through KW6 in **Fig. 9**. The effects of the geometry may be checked by performing the measurements simultaneously at several different points where the water depth and soil profile are the same. Provided that the water depth does not change drastically, the power spectra of the pressure observed at the different points at the same time should be equal. If a significant difference is observed, it is an indication that there is some significant effects of the geometry such as the refraction from the seawall. In a real application of the BSMP, usage of two or more BSMPs at the same time will tell us if there is any effects of the geometry.

The comparisons of the shear modulus profiles among the points KW1, KW2 and KW4, where the soil profiles have been found almost identical, are shown in **Fig. 18**. The values of the shear modulus decrease for the points further away from the seawall. This is beacause the seabed motion of the points close to the seawall are somewhat more restrained than those sway from the wall. Point KW1 is located about 44 meters from the seawall whereas the distance of point KW4 is about 175 meters from the seawall (see **Fig. 9**). In order to clarify this point, one may compare the pressure and the power spectra of the seabed motion at points KW1, KW2 and KW4. **Figs. 19(a)** and **19(b)** show the seabed pressures and vertical seabed motion for points KW1, KW2 and KW4, respectively. The power spectra for pressures seem to vary slightly among them and the peak amplitude of the displacement increases as we move from point KW1 to KW4. These changes may be attributed to the combination of scattered and reflected waves and the distance of the experi-

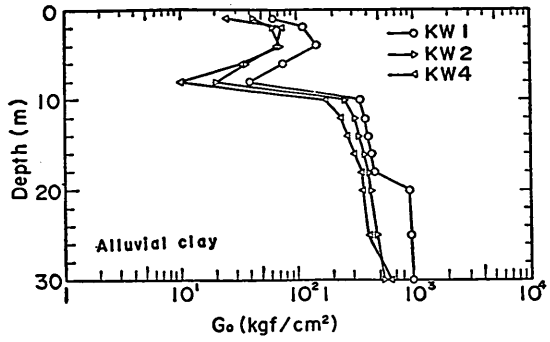

Fig. 18 Shear modulus profiles measured at different points KW1, KW2 and KW4

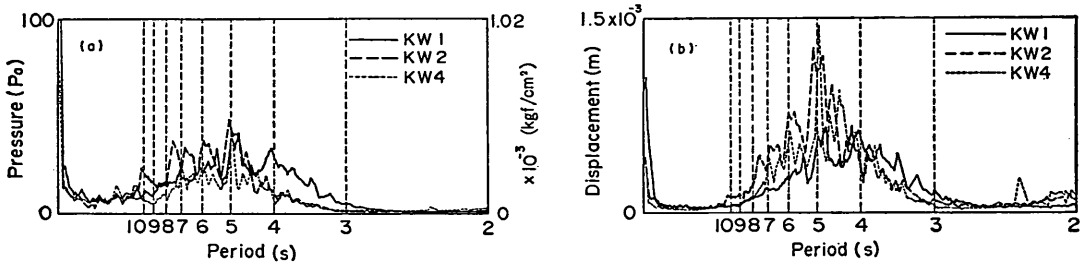

Fig. 19 Power spectra; (a) water pressures, (b) seabed motion

ment point from the seawall. The shear modulus valves of the point KW4 are also much closer to the laboratory and DM values than those of points KW1 as previously shown in **Fig. 15**. It is considered that the results may be bias for the points close to the seawall.

The above discussion seems to be the cause of discrepancies of the shear mobulus between the BSMP and other measurements. The discrepancies due to the geometrical reason are, however, not so large as those due to the different measurements adopted in this study. This can be understood by comparing **Fig. 18** with **Fig. 15**.

5. Concluding Remarks

The shear modulus profiles were measured with the Bottom Shear Modulus Profiler (BSMP) and compared with those evaluated from other in-situ and laboratory methods such as the Downhole Method (DM), Standard Penetration Test (SPT), Unconfined Compression Test (UCT) and Cyclic Triaxial Test (CTT). The advantages of the BSMP technique are that the measurement itself takes only a couple of hours and the analysis of the data give an estimate of the quantitative shear modulus. Even at a site with a water depth of 100m, the measurement is basically the same as that with a 10m depth if restrictions in the application of the BSMP are made clear. These advantages will be appreciated in many surveys of the seabed structure.

The main findings obtained from this study are summarized as follows:

(1) The shear modulus of the sand layer measured with the BSMP indicated a fairly

good agreement with those obtained from the DM and SPT results.

(2) The agreements of the shear modulus profiles of the alluvial clay layers estimated from the BSMP and DM were good in the shallow depths of less than 10m. Whereas, the shear moduli evaluated from the UCT and CTT were a little smaller than those measured with the BSMP.

(3) The BSMP data under such wave conditions as observed in this field experiment gave slightly larger shear moduli than those obtained from other measurements, especially at the deep clay layer.

(4) It was found that the discrepancies of the shear modulus profiles due to the geometrical reason were not so large as those due to the differences of the measurements adopted in this study.

(*Received on Septenber 17, 1990*)

Acknowledgments

The authors wich to thank the members of the Second District Port Construction Bureau of the Ministry of Transport, Japan, for their help in the data collection at the port of Kawasaki. Dr. Tsuchida, the Director General of PHRI, is highly appreciated for his kind assistance extended to the first author during his stay in Japan. This project was made possible through a post doctoral fellowship from the Science and Technology Agency of Japan.

References

1) Aki, K. and Richards, P. G.; "Quantitative Seismology: Theory and methods", Vols. 1 and 2, W. H. Freeman, New York, 1980.
2) Badiey, M., Yamamoto, T. and Turgut, A.; "Laboratory and in situ measurements of selected geoacoustics properties of carbanate sediments", *J. Acoust. Soc. Am.*, Vol. 84, No. 2, pp. 689-696, 1988.
3) Badiey, M., Yamamoto, T. and Turgut, T.; "Laboratory measurements of geo-acoustics profiles of the New Jersey Shelf sediments", *J. Acoust. Soc. Am.*, Suppl. 1, Vol. 81, pp. S49, 1987.
4) Cox, C., Deaton, T., and Webb, S., "A deep-sea differential pressure gauge", *J. Atm. and Oceanic Tech.*, Vol. 1, No. 3, 1984.
5) Ishihara, K.; "Fundamental Soil Dynamics", Kashima Shuppankai, Tokyo, 1976 (in Japanese).
6) MacLamore, V. R., Anderson, D. G. and Espana, C.: "Crosshole Testing Using Explosive and Mechanical Energy Sources", *Dynamic Geotechnical Testing*, ASTM, STP 654, pp. 30-55, 1978.
7) Ohsaki, Y. and Iwasaki, R.; "On dynamic shear moduli and poison's ratios of soil deposits", *Soils and Foundations*, Japanese Soc. Soil Mech. and Foundation Eng., Vol. 13, No. 4, pp. 61-73, 1973.
8) Okumura, T.; "Studies on the disturbance of clay soils and the improvement of their sampling techniques", *Technical Note of the Port and Harbour Reseach Instiute*, No. 193, p. 145, 1974 (in Japanese).

9) Richart, F., E., Hall, J., R. and Woods, R. D.; "Vibration of soil and foundations", Prentice-Hall, Englewood Cliffs, NJ, 1970.
10) Seed, H. B. and Idriss, I. M.; "Soil moduli and damping factors for dynamic response analysis", *Rep. No. EERC 70-10*, University of California, Berkeley, 1970.
11) Suzuki, H., Yamamoto, T. and Badiey, M.; "Seabed shear modulus measurement by use of gravity water waves", *J. Acoust. Soc. Japan*, Vol. 46, No. 1, pp. 68-73, 1990 (in Japanese).
12) Trevorrow, M., Badiey, M., Turgut, A., Conner, C., and Yamamoto, T.; "A quantitative analysis of seabed shear modulus from experiments on the New Jersey Shelf in August 1986", *RSMAS Technical Report*, University of Miami, TR-87-003, GAL Report 1003, 1987.
13) Trevorrow, M., Yamamoto, T., Badiey, M., Turgut, A. and Conner, C.; "Experimental verification of seabed shear modulus profile inversions using gravity (water) wave-induced seabed motion", *Geophysical Journal*, Vol. 93, No. 3, pp. 419-436, 1988.
14) Yamamoto, T.; "Numerical integration method for seabed response to water waves", *J. Soil Dynam. and Earthq. Engr.*, Vol. 2, No. 2, pp. 92-100, 1983a.
15) Yamamoto, T.; "Propagator matrix for continuously layered porous seabeds", *Bull. seism. Soc. Am.*, Vol 73, pp. 1599-1620, 1983b.
16) Yamamoto, T. and Torii, T.; "Seabed shear modulus profile inversion using surface gravity (water) wave-induced bottom motion", *Geophys J. R. Astrom. Soc.*, Vol. 85, pp. 413-431, 1986.
17) Yamamoto, T., Trevorrow, M., Badiey, M., and Turgut, A., "Determination of the seabed porosity and shear modulus profiles using a gravity wave inversion", *Geophys. J. Int.*, Vol. 98, No. 1, pp. 173-182, 1989.
18) Zen, K., Yamazaki, H. and Umehara, Y,; "Experimental study on shear modulus and damping ratio of natural deposits for seismic response analysis", *Report of the Port and Harbour Research Institute*, Vol. 26, No. 1. pp. 41-113, 1987 (in Japanese).

Notations

a, b : experimental constants
d : thickness of the bottom layer
e : void ratio
f : frequency
G_{intt} : initial shear modulus profile
G_m : shear modulus of the mth layer
G_o : shear modulus at the low amplitude of shear strain
G_o (lab.) : G_o measured in the laboratory
G_o (in-situ) : G_o measured at the field
G_s : specific gravity
$G(z)$: shear modulus as a function of depth
h : water depth
I_p : plasticity index
K_o : coefficient of earth pressure at rest
N : number of blows in the SPT
$P(z)$: water pressure as a function of depth
q_u : unconfined compressive strength
r : displacement-stress vector

S_{aa} : autopower spectrum of acceleration
S_{pp} : autopower spectrum of pressure
S_{pa} : crosspower spectrum of pressure and acceleration
S_r : degree of saturation
u : horizontal displacement
V_s : shear wave velocity
v : vertical displacement
w : water content
x : horizontal coordinate
z : vertical coordinate
γ : coherence function
γ_t : unit weight of soil
ε_f : axial strain at failure
λ : wave number
$\xi\ (f)$: admittance as a function of frequency
ξ_n : admittance of the nth wave
σ'_c : effective confining pressure
τ_{xz} : shear stress
ω : angular frequency